ICANS-XI International Collaboration on Advanced Neutron Sources
KEK, Tsukuba, October 22-26, 1990

THERMAL-HYDRAULICS INVESTIGATIONS FOR THE LIQUID LEAD-BISMUTH TARGET OF THE SINQ SPALLATION SOURCE

B. Sigg, Swiss Federal Institute of Technology, Nuclear Engineering Laboratory
T. Dury, M. Hudina, B. Smith, Thermal-hydraulics Laboratory

Paul Scherrer Institute, 5232 Villigen, Switzerland

Abstract

The paper contains a discussion of the thermal-hydraulic problems of the target which require detailed analysis by means of a two- or three-dimensional space- and in part also time-dependent fluid dynamics code. There follows a short description of the general-purpose code ASTEC, which is being used for these investigations, and examples of the target modelling, including results. The final part of the paper is devoted to a short discussion of experiments against which this application of the code has to be validated.

1 Introduction

In an earlier phase of the project, thermal-hydraulics analysis of the SINQ Liquid Lead-Bismuth Target was mainly based on experimental investigations and simplifying engineering calculation methods [1,2,3]. Later, it was found that detailed computations of the fluid dynamic phenomena had to be undertaken, in order to adequately predict temperature distributions and resulting thermal stresses occurring in the target structures, under all kinds of operational conditions. This applies mainly to the target windows, because recently detected uncertainties with respect to the proton beam profile require accurate predictions of thermal stresses to be made for cases of extreme thermal load.

2 Target description

The reference target of the SINQ Spallation source consists of a vertical liquid lead-bismuth-eutectic (LBE) column contained in a chromium-steel vessel (see Fig.1). The proton beam enters the target through a triple-walled window from below and deposits its energy mainly within the lower 0.3 m of the target. For a nominal beam current of 1.5 mA, a thermal power of 650 kW has to be removed. This is done by natural circulation of the LBE, which rises through a central guide tube to the top of the liquid column and then descends via a heat exchanger, situated in the annulus of the target container. The heat exchanger consists of a cluster of 24 water-cooled pins, distributed uniformly in the annulus. Water enters a pin by flowing down inside an inner tube and exits via the pin annulus. The closure arrangement at the bottom of the target consists of a lower, double-walled safety window, cooled internally by water, and an upper, cusp-shaped window, cooled by the LBE itself (see Fig.2). Further details on window design are given in [4]. Natural circulation within the target is not generated solely by the proton beam itself. During beam shut-down, electrical heater rods, with a total power of 40 kW and which are installed inside the guide tube above the beam-heated region,

cause sufficient pre-circulation of the target liquid to allow the proton beam to be started up within about 20 seconds.

Fig.1 also shows auxiliary heating/cooling ducts for melting/freezing of the LBE. For the transfer of the target to a near-by repository, the LBE will be solidified to reduce transportation risks. Further technical data can be found in Table 1.

3 Thermal-hydraulics problems of the target arising during normal operation, transients and malfunctions

The thermal-hydraulics problems of the target are mainly related to the task of ensuring integrity of the windows under all operating conditions, which means demonstrating that thermal stresses and temperatures remain within safe limits. The main source of concern lies in the variability of the proton beam profile. This is caused by the requirements of the users of Target E, a meson target which lies upstream in the beam channel, and by imperfect reliability of the beam control system. For the window region of the SINQ target the proton beam current density can be considered a combination of the following two, roughly Gaussian, distributions:

$$j(r) \approx \frac{J_1}{\pi\sigma_1^2}\, e^{-\frac{r^2}{\sigma_1^2}} + \frac{J_2}{\pi\sigma_2^2}\, e^{-\frac{r^2}{\sigma_2^2}} \qquad (1)$$

where: J_1, J_2 = total currents of components, with $J_1 + J_2 = 1.5$ mA
$\sigma_1^2 = 1.8$ cm^2
$\sigma_2^2 = 19$ cm^2
r = Radius from beam axis.

The first term in (1) is due to protons by-passing Target E and the second to protons scattered in Target E.

If it was possible to guarantee window integrity during continuous operation with the full beam being unscattered by Target E, this would, of course, considerably simplify the target safety issue. For the design calculations, the preliminary assumption has been made that the peaked part of the beam contributes one third of the total beam, i.e. $J_1 = 0.5$ mA.

There are, of course, other parts of the target container where thermal-stress problems could arise, e.g. in the structures around the window, the lower portion of the guide tube, and the entry section of the pin coolers, where hot LBE with an undulating free surface flows by and causes thermal stressing in the walls. Additional stress problems are brought about by normal operational transients and exceptional situations due to special malfunctions. Details on window design and stress analysis calculations can be found in [4] and [5].

Table 2 presents a summary of cases which have to be analysed by means of thermal-hydraulic and stress calculations. These computations have to be repeated, if necessary, in the course of an optimisation of the target geometry (Window shape, materials of the guide tube, its distance from the window and shape at the bottom edge, geometry of pin coolers, etc.).

Adequate solutions to the resulting thermal-hydraulic calculational problems can only be obtained by means of advanced fluid dynamics codes which have the ability to solve the two- and three-dimensional, steady-state and time-dependent thermal-hydraulic differential equations in complex geometry. Beside geometrical complexity, there are a number of thermal-hydraulic phenomena which warrant the use of such a code:

1) On the window surface an internally-heated boundary layer develops. Together with the power density and geometry of the window, the velocity distribution within this layer, its thickness and its turbulent structure will determine the window temperature distribution. These properties deviate from those of

an ordinary plane boundary layer because of buoyancy forces, surface curvature and flow geometry (converging flow).

2) Behind the lower edge of the guide tube and, under special conditions, also on the surface of the window, flow detachment can occur.

3) During transients, other buoyancy-induced flow distributions may form above the window which can give rise to different window cooling behaviour. This is of particular importance for start-up transients with inadequate pre-circulation.

4) For the investigation of safety-relevant incidents, it is preferable to be able to make best-estimate calculations instead of having recourse to worst-case analyses.

The ASTEC code [6,7] was chosen to perform the necessary calculations because of its flexibility and its proven ability in solving natural convection problems [8]. Additionally, our special contacts with the code developers will guarantee good support in the event of code-running difficulties.

4 Short description of ASTEC

ASTEC solves, in general, a porous-medium form of the thermal-hydraulic, time-dependent partial differential equations in a finite volume approximation [6,7]. Fluids may be compressible or incompressible, and there is an option for the solution of additional mass transport equations. For incompressible fluids, ASTEC treats the thermal-hydraulics equations in the Boussinesq approximation. In regions of turbulent open flow (no porous medium), ASTEC solves, if required, the $k - \varepsilon$ turbulence model transport equations in order to determine space-dependent turbulent viscosities and diffusivities.

The finite-volume approach combines the flexibility of the finite-element method with the numerical stability of finite difference schemes. It allows one to subdivide the three-dimensional solution domain into hexahedra (8-node elements) of arbitrary shape. Finite volumes are formed around the corner points (nodes) according to a special geometrical procedure (see Fig.3). For the purpose of the numerical approximation, all variables are discretised at the nodes, except pressures, which are stored at the element centres.

The time-dependent discretised equations are solved by means of the time-implicit SIMPLE algorithm [9], adapted to the finite-volume arrangement of grid points. A hybrid skew-upwind scheme is optionally used for the advection terms to reduce false diffusion. Steady-state solutions are obtained by calculating a "false" transient, using very large time steps.

The code has a number of features which allow complicated problems to be solved:

- Several disconnected fluid regions with different material properties are possible.
- Heat transfer between fluids and solids may be modelled by prescribed heat transfer coefficients, if the code is not to perform an explicit boundary layer calculation.
- Additional modelling can be implemented using Fortran subroutines supplied by the user.
- The programming is adapted to vector-processing machines, an advanced version also to transputers.
- Packages for interactive pre- and post-processing (mesh generation, data analysis) are available.

ASTEC has been validated against some benchmark cases and the natural-convection experiment SONACO, which was performed at PSI [6,8,10].

5 Some results of ASTEC calculations for the SINQ-target

An ASTEC model of the target is shown in Figs. 4+5. It consists of a 22.5^0 sector of the cylindrical target, the smallest sector which allows explicit modelling of the pin coolers. Each face of the wedge model is a plane of symmetry. The central downflow-tube of the pin coolers is simulated by an annulus for simplicity, and heat transfer across the inner tube (water-to-water heat exchange) is modelled by means of heat transfer coefficients. For locations within the LBE itself, the meshing near surfaces is made sufficiently fine for the code to resolve the thermal boundary layer. The model shown in the figures has 9420 nodes and 7906 elements, and the cpu time needed to complete calculation of a stationary case is about 2-3 hours on the Cray-2 of ETH Lausanne.

In a first series of calculations, effects of window shape and guide tube insulation were investigated. Figs. 6-9 compare results of velocity and temperature distributions for a domed and a cusp-shaped window. Obviously, the latter must receive much better cooling near the target axis, since window temperatures near the centre are found to be much lower than for the domed window. In both cases no flow detachment occurs on the window surface itself, but a zone of recirculating flow forms inside the bottom end of the guide tube. Maximum velocities rise from about 0.6 m/s in the case of the domed window to about 0.7 m/s for the cusped one.

The one-third fraction of the beam reaching the SINQ target unscattered is responsible for the high window temperatures in the centre. When the full beam is diffuse, maximum temperatures for the domed window are reduced by about 400^0C.

Temperature distributions along the axis of the target show a rapid drop from the window into the fluid and a subsequent increase due to volumetric heating (see Figs. 10+11). The large temperature difference between the window surface and the relatively cool fluid layer above illustrates the importance of proper fluid flow and heat transport modelling in the boundary layer.

Using an insulating instead of a thermally conducting guide tube leads to somewhat lower temperatures in the window region ($\approx 20^0$C less) and to a slightly higher LBE circulation rate. Figs. 12+13 compare the axial temperature distributions on the outside surface of the guide tube for cases with thermally-conducting and insulated wall, respectively. The effect does not seem to be important enough to justify the resulting material and shielding complications caused by employing an insulating guide tube, although it must be said that heat exchange between the riser and the annulus leads to mixed-convection flow effects, i.e. slightly higher turbulent heat exchange and friction. Since buoyancy forces near the guide tube oppose the overall circulation forces, however, no problems with discontinuity of heat transfer coefficients and friction factors occur as in the case of buoyancy-aided flow [11].

In Figs. 14+15 temperature distributions around the pin circumference and in a cross-section of the annulus near the bottom of the cooling pins are shown. The variations around pins are not excessive and should not give rise to thermal-stress problems. The transverse temperature distribution at the bottom of the bundle shows that a current of relatively warm liquid issues from the subchannels between the inner pin coolers, whereas overcooled liquid exits near the outer wall. The arrangement of the pins could be somewhat better optimised, although the overall efficiency of the cooling arrangement seems to be acceptable. In the calculation there were 8 pins in the innner ring and 16 in the outer. A 9/15 arrangement could enable the pins to be more uniformly spaced in the annulus, though this geometry would increase the number of meshes needed for the ASTEC model. In addition, it is questionable whether such an arrangement could noticeably improve the cooling efficiency beyond that of an optimised 8/16 configuration.

Further ASTEC calculations are in preparation. These use a finer mesh near the centre of the window, to reduce discretisation errors in the temperature field computation. Transient calculations to investigate time-dependent window temperature distributions for the analysis of transient stresses are also in progress. They

will be carried out on a restricted window-region model, with prescribed velocity distribution at the inlet to avoid excessive computer time.

6 Benchmark experiments

Although ASTEC has been validated against a number of experiments [6,8,10], additional testing of the code on experiments closely related to the SINQ target geometry is considered necessary.

The first benchmark is to be the half-scale mock-up test of the target described in [12]. Its results will serve to test ASTEC with respect to integral performance, i.e. circulation rate, transient behaviour, and heat transfer to coolers.

A second experiment, called TACOS (Target Cooling Simulation), is intended to compare ASTEC calculations with measured temperature and velocity distributions in the window region. The experiment simulates flow conditions above the window and heat transfer from the window surface to the LBE stream but does not include volumetric heating. Sodium has been chosen as the simulant fluid, because of the possibility of performing the experiment in a new on-site sodium loop. The design of the TACOS test section is shown in Fig.16. It will allow the exchange of the heated part of the window as well as the lower end of the guide-tube, and variation of the distance between the bottom of the guide tube and the window. Temperature measurements will be made by means of themocouples above and below the window membrane, on the tips of a movable rake, and at various positions along the walls. Movable permanent-magnet velocity probes will enable measurements of velocity profiles to be made across the annulus and riser. There are two inlet chambers to the test section, allowing asymmetric flow distributions across the window to be generated.

The auxiliary heaters below the inlet chambers are needed for the production of temperature fluctuations. These are intended to be used in correlation analyses for determining the circumferential flow distribution in the annulus.

The setting-up of this special TACOS experiment for the testing of ASTEC is necessary because of the complicated fluid dynamic phenomena occurring in the window region, and by the strong influence which the window shape exerts on the temperatures, as exemplified by the results of ASTEC for the domed and cusped windows.

7 Conclusions

The complicated geometry of the SINQ target and the high heat load to which the target windows are exposed warrant the use of the advanced, thermal-hydraulics code ASTEC.

First results show the importance of optimising the window geometry, but more refined calculations are still needed to give better details of window temperature distributions near the central axis.

Additional benchmarking of the code, as described in the paper, is recommended in order to test its integral performance and particularly its ability to adequately predict temperatures in the window region of the target.

References

[1] Ch. Tschalär: Proc. ICANS-V, Jülich 1981.

[2] Y. Takeda: Proc. ICANS-VII, Chalk River 1984, AECL 8488.

[3] Y. Takeda: Proc. ICANS-IX, Villigen 1986.

[4] M. Dubs, J. Ulrich: These proceedings.

[5] G. Heidenreich: These proceedings.

[6] R.D. Lonsdale, R. Webster: The application of finite volume methods for modelling three-dimensional incompressible flow on an unstructured mesh.
Proceedings of 6th International Conference on Numerical Methods in Laminar and Turbulent Flow, Swansea, July 1989.

[7] R.D. Lonsdale: ASTEC, Release 1.7B: Users Manual, 14th Nov. 1989, AEA Technology, Dounreay.

[8] G. Robinson, R.D. Lonsdale, T.V. Dury: Comparisons between experimental results and numerical simulations for the SONACO sodium natural convection experiments. Proc. of the 4th Int. Conf. on Liquid Metal Engineering and Technology, 17-21 Oct. 1988, Avignon, Vol.2, p.411.

[9] S.V. Patankar: Numerical Heat Transfer and Fluid Flow. Hemisphere Publ. Corp. 1980.

[10] R.D. Lonsdale: An Algorithm for Solving Thermal-Hydraulic Equations in Complex Geometries: The ASTEC Code.
Int. Top. Meetg. on Adv. in Reactor Physics, Math. and Computation, April 27-30, 1987, Paris.

[11] M.A. Cotton, J.D. Jackson: Comparison between Theory and Experiment for Turbulent Flow of Air in a Vertical Tube with Interaction between Free and Forced Convection. ASME Winter Annual Meeting 1987, Symposium on Combined Free and Forced Convection.

[12] Y. Takeda, W.E. Fischer: These proceedings.

Table 1: Characteristics of SINQ-target

Geometry (see also Fig.1)

Height of LBE column: 3343 mm
Outer diameter in moderator region: 180 mm
Outer diameter in pin cooler region: 370 mm

Thermal-hydraulics:

Target fluid:
Thermal power with nominal beam (1.5 mA) P = 650 kW
LBE circulation rate $M \approx 37$ kg/s

Pin coolers:
Water inlet temperature $T_{in} = 128\ ^{0}C$
Water outlet temperature $\overline{T_{out}} = 147\ ^{0}C$
Total flowrate $\dot{M} = 8.0$ kg/s
Total number of pins: 24

Table 2: Normal and safety-related operational conditions of target to be investigated

1) Stand-by operation:
   - Pre-circulation by auxiliary heaters
2) Start-up transients:
   - Normal beam power ramp
   - Too-steep ramp
   - Narrow-beam ramp
   - Beam start-up with insufficient pre-circulation
   - Restart of cooling after overheating incident
3) Full-power operation
   - Design case
   - Too-large fraction of beam by-passing Target E
   - Failure of secondary cooling
   - Impeded circulation due to guide tube defects or loose parts
   - Rupture of water-cooled safety window causing water spray on lower surface of LBE window
4) Shut-down transients
   - Normal case
   - After beam control malfunction or operator error (beam profile, start-up ramp)
   - After insufficient cooling
   - After failure of safety window.

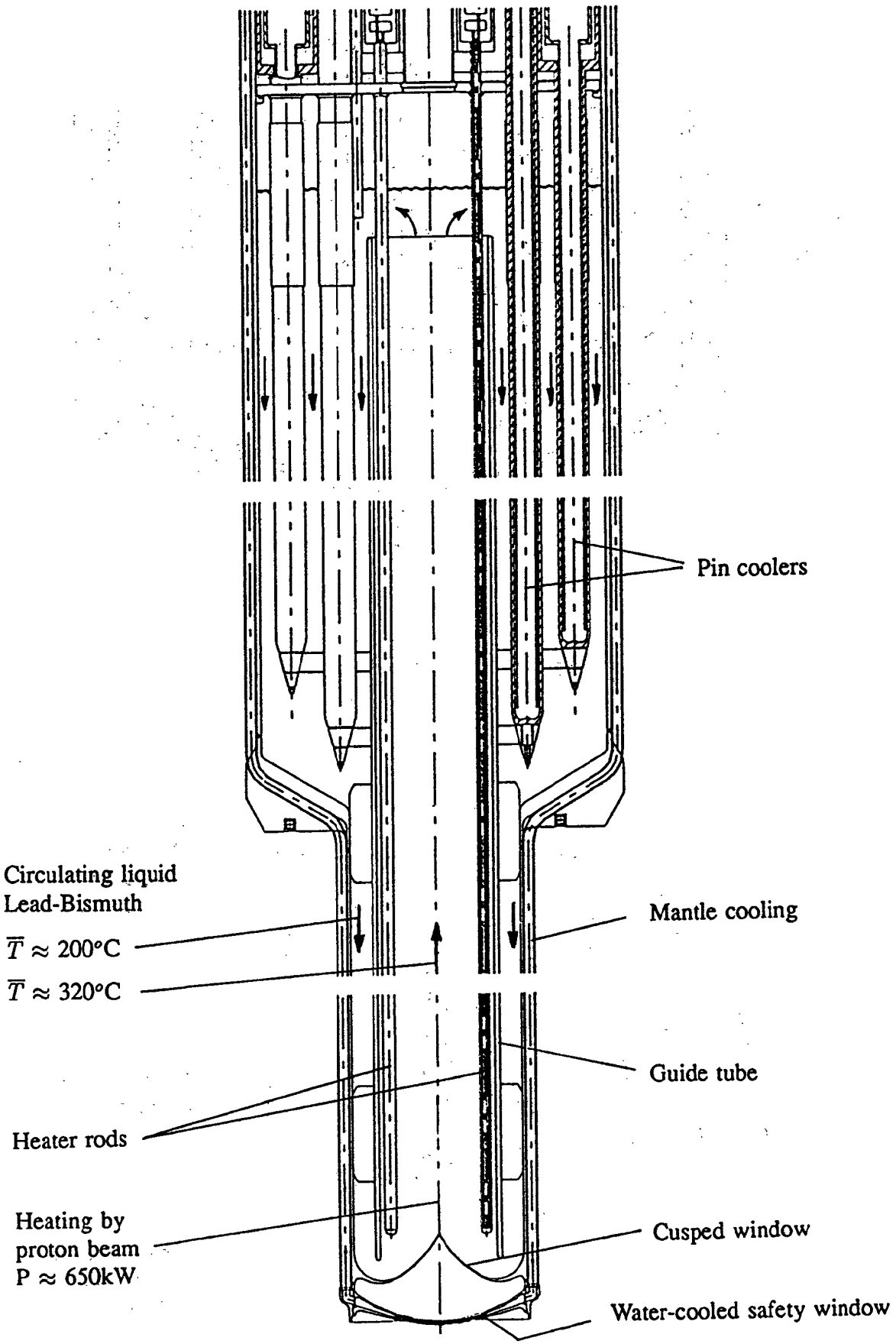

Fig.1 Sketch of SINQ target

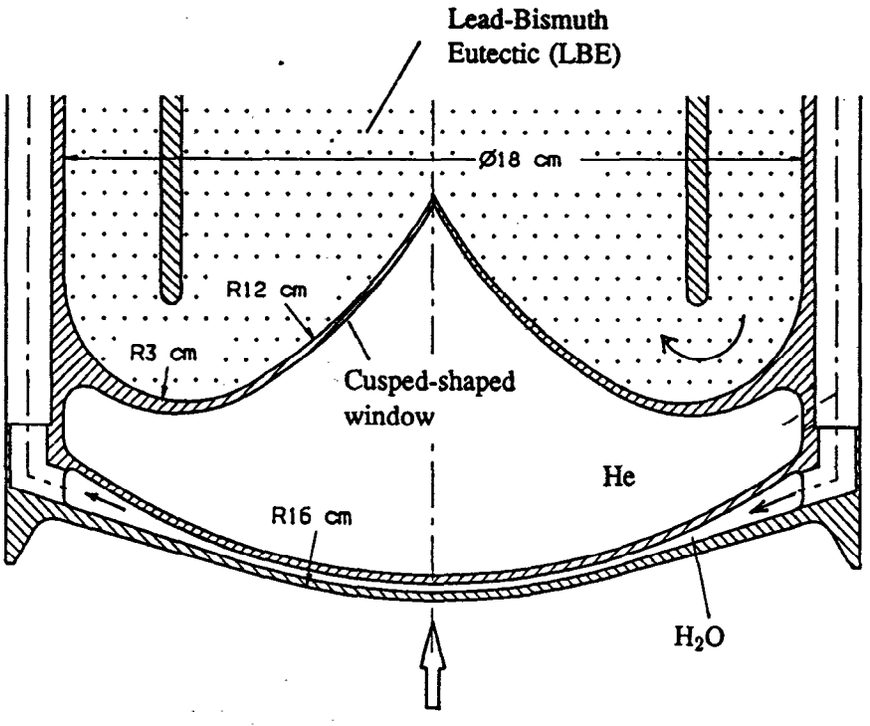

Fig.2 Cusp-shaped window design

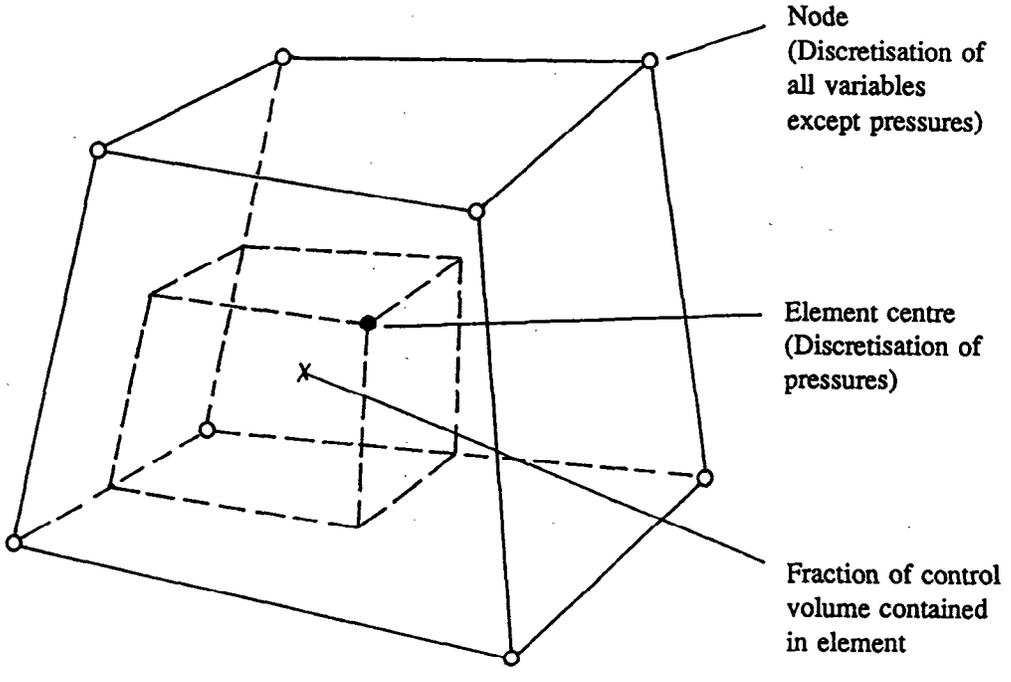

Fig.3 An 8-node element used for 3d meshes

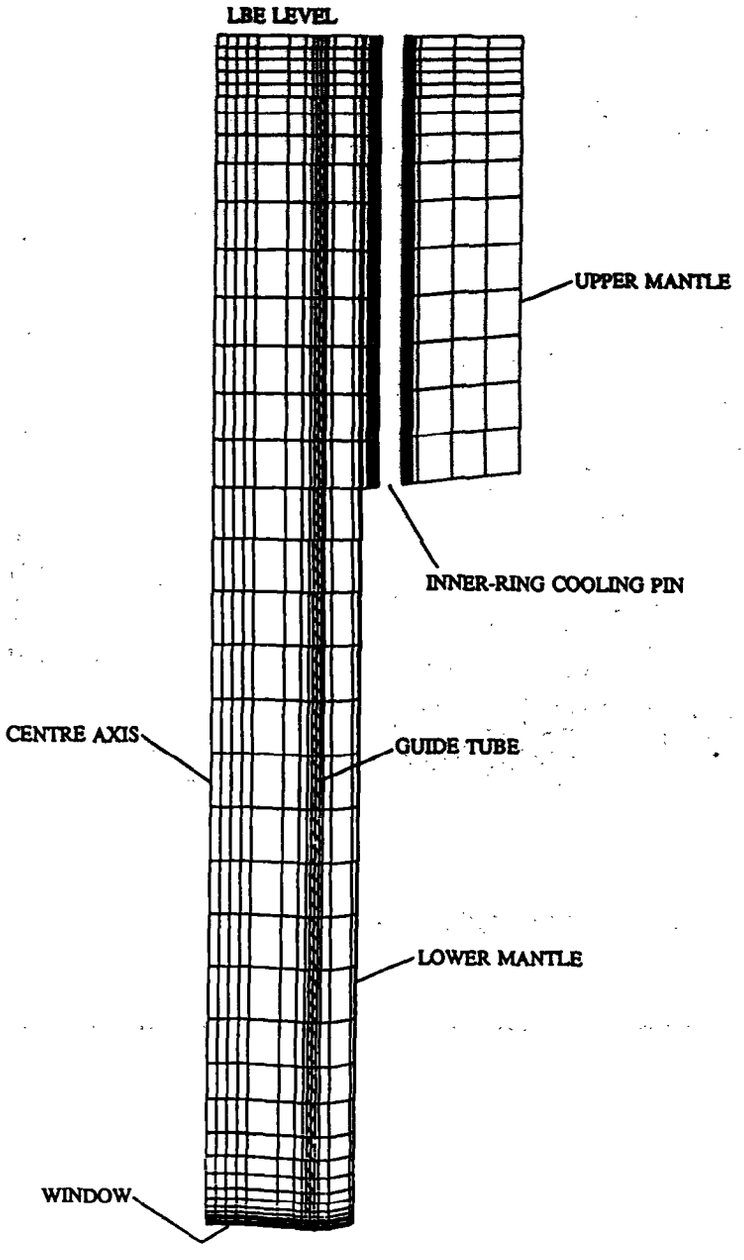

Fig.4
ASTEC target model - side view (domed window)

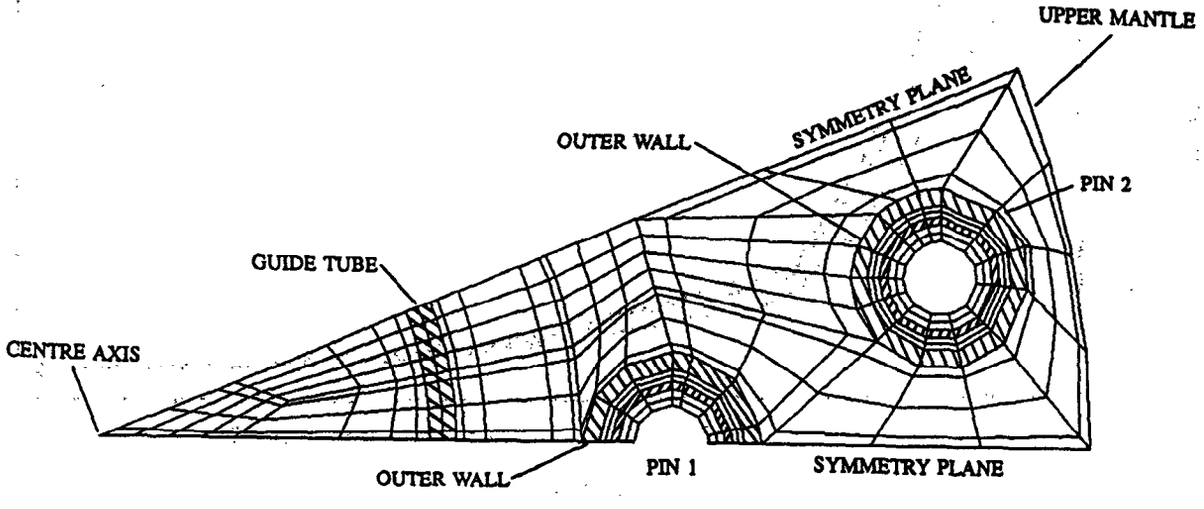

Fig.5 ASTEC mesh - Plan view of top plane

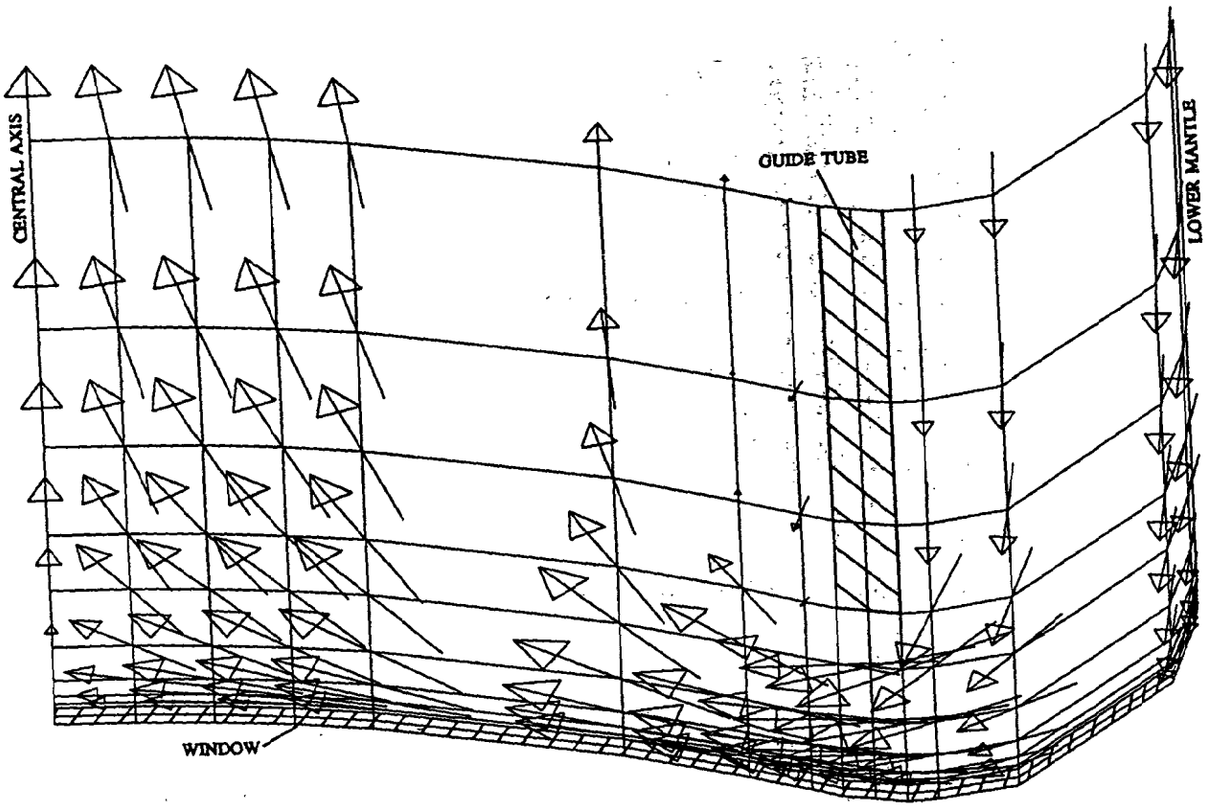

Fig.6 Domed window - velocity distribution above window

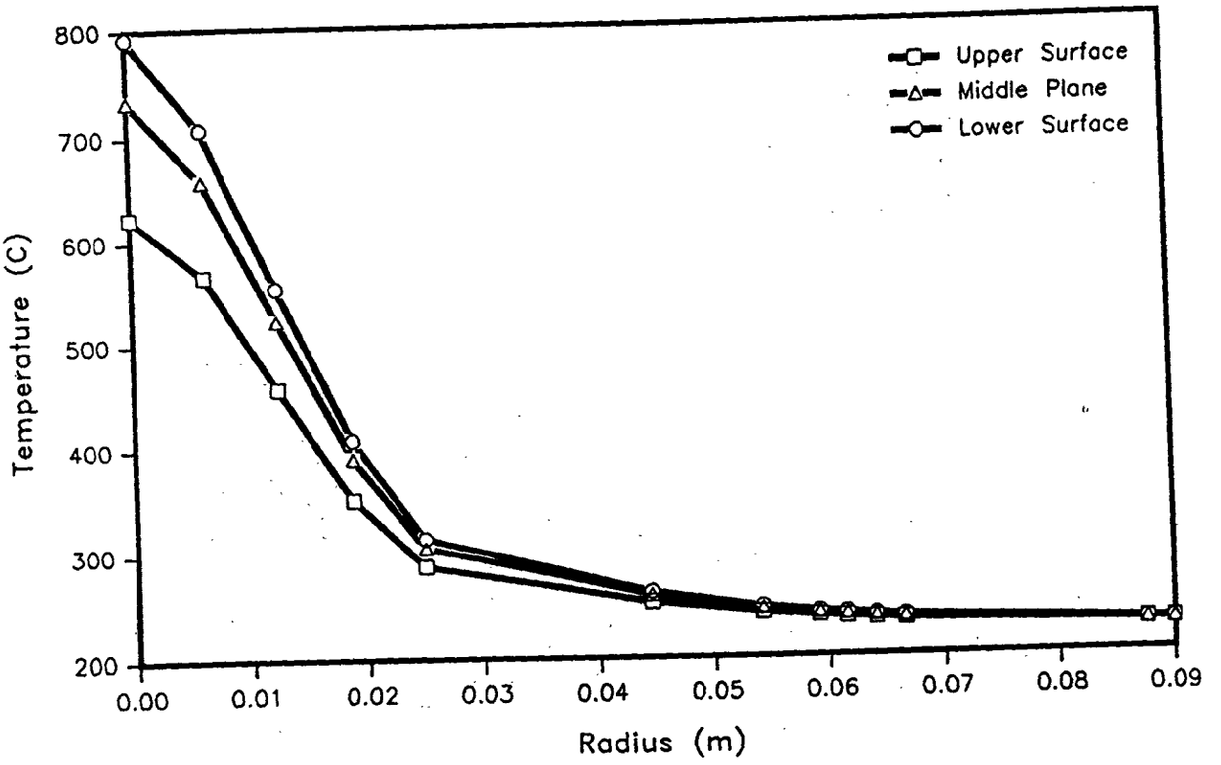

Fig.7 Domed window - Temperature distribution in window

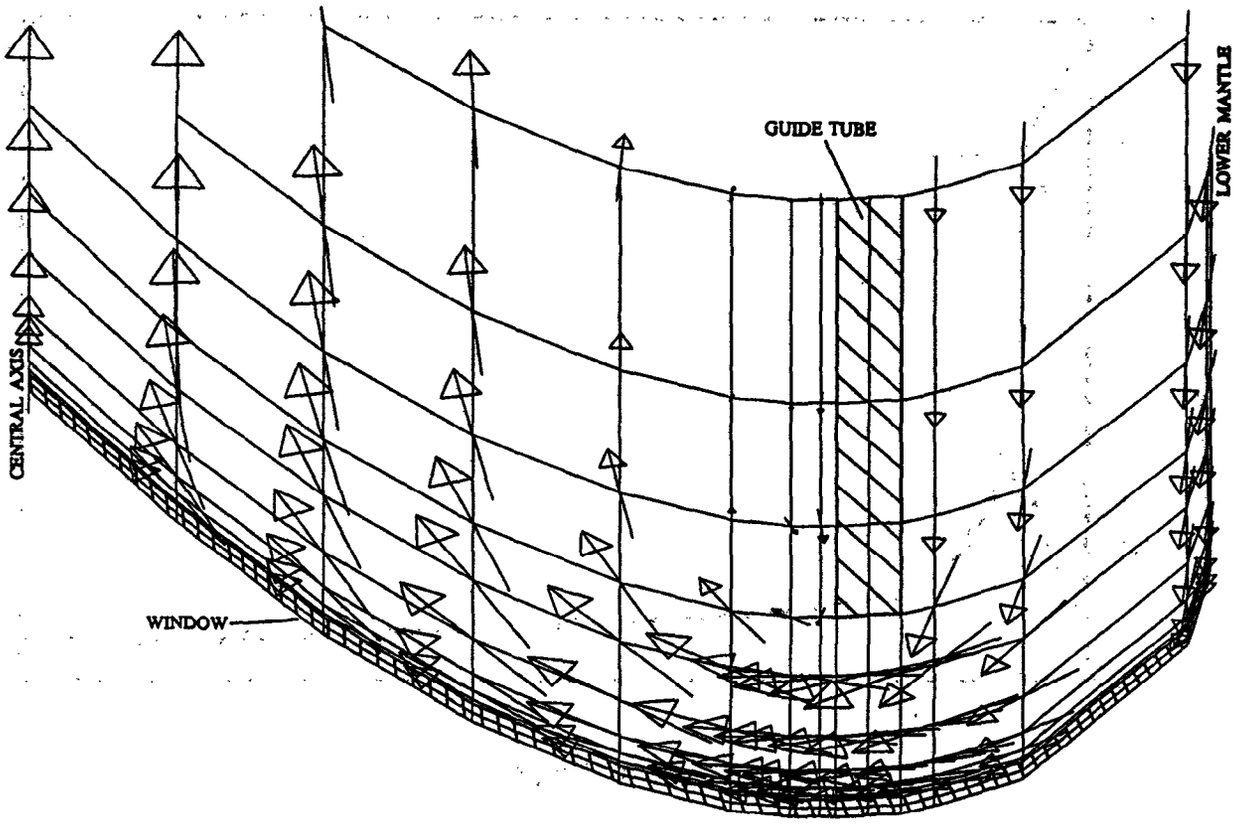

Fig.8 Cusped window - Velocity distribution above window

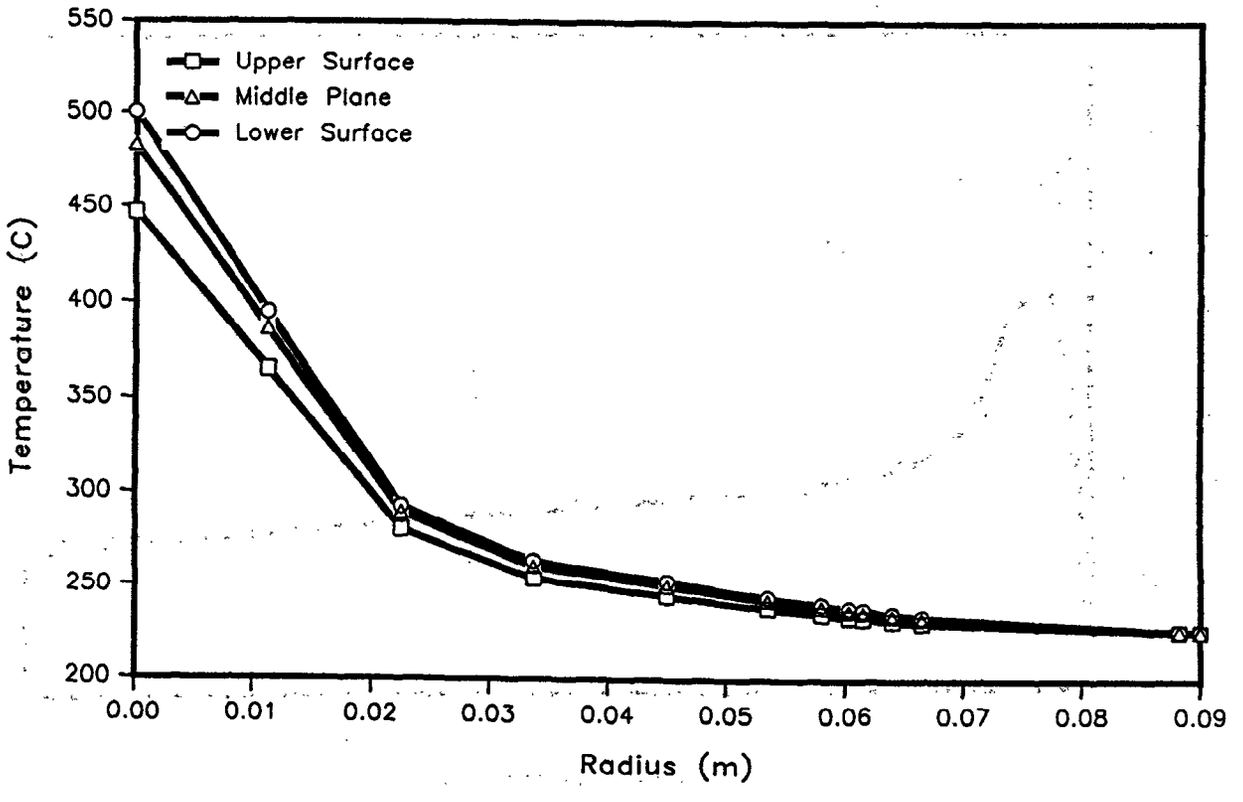

Fig.9 Cusped window - Temperature distribution in window

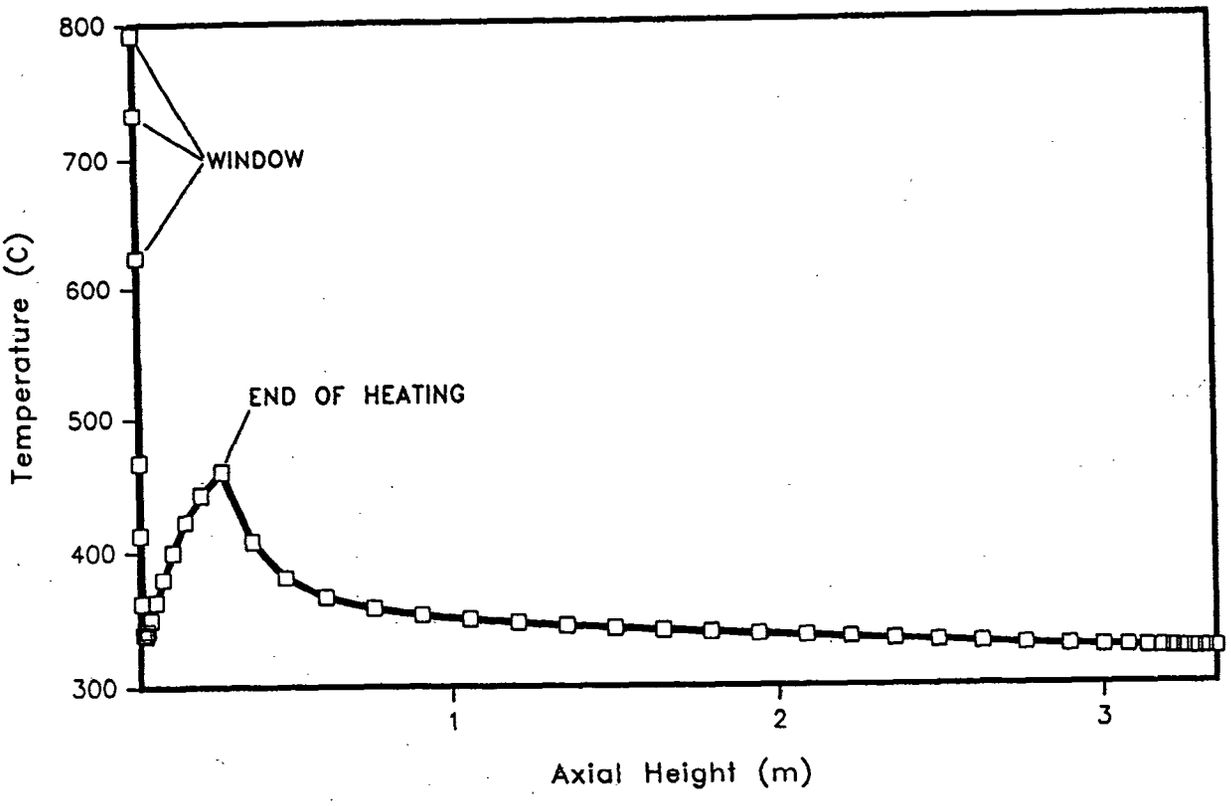

Fig.10 Domed window - Temperature distribution along target axis

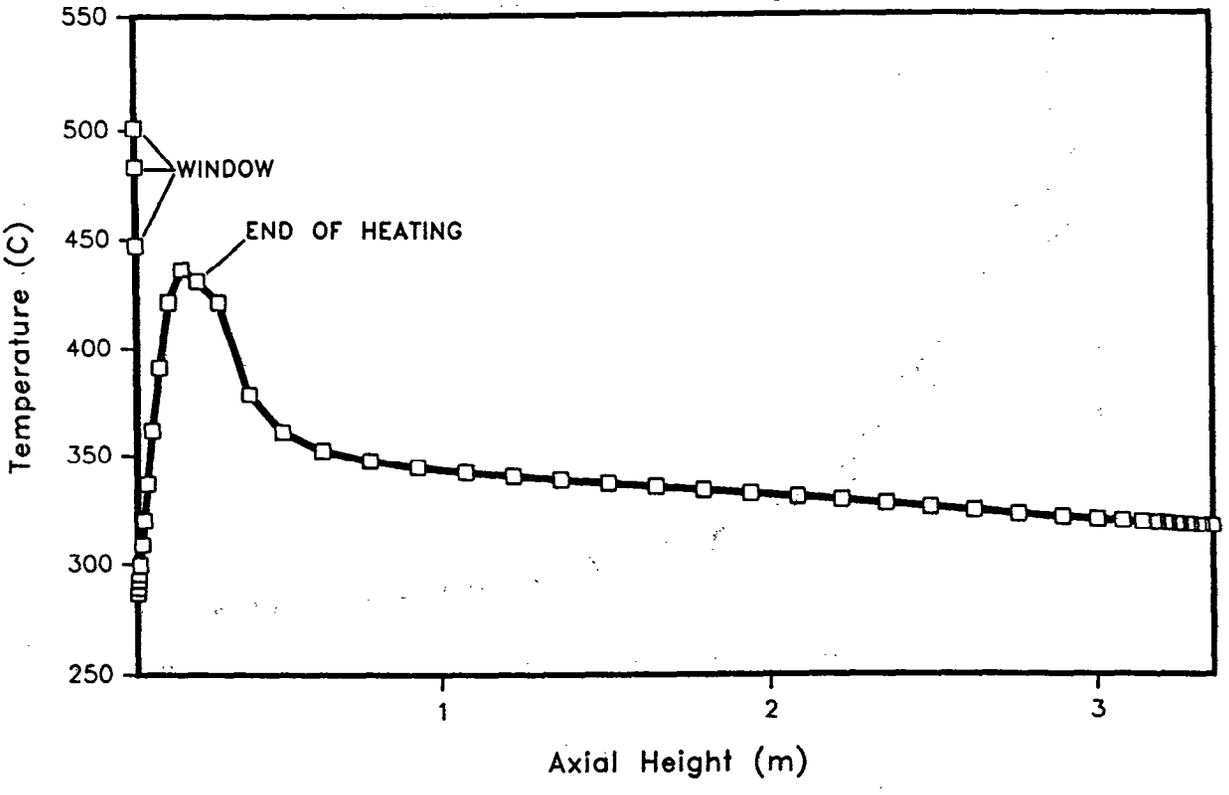

Fig.11 Cusped window - Temperature distribution along target axis

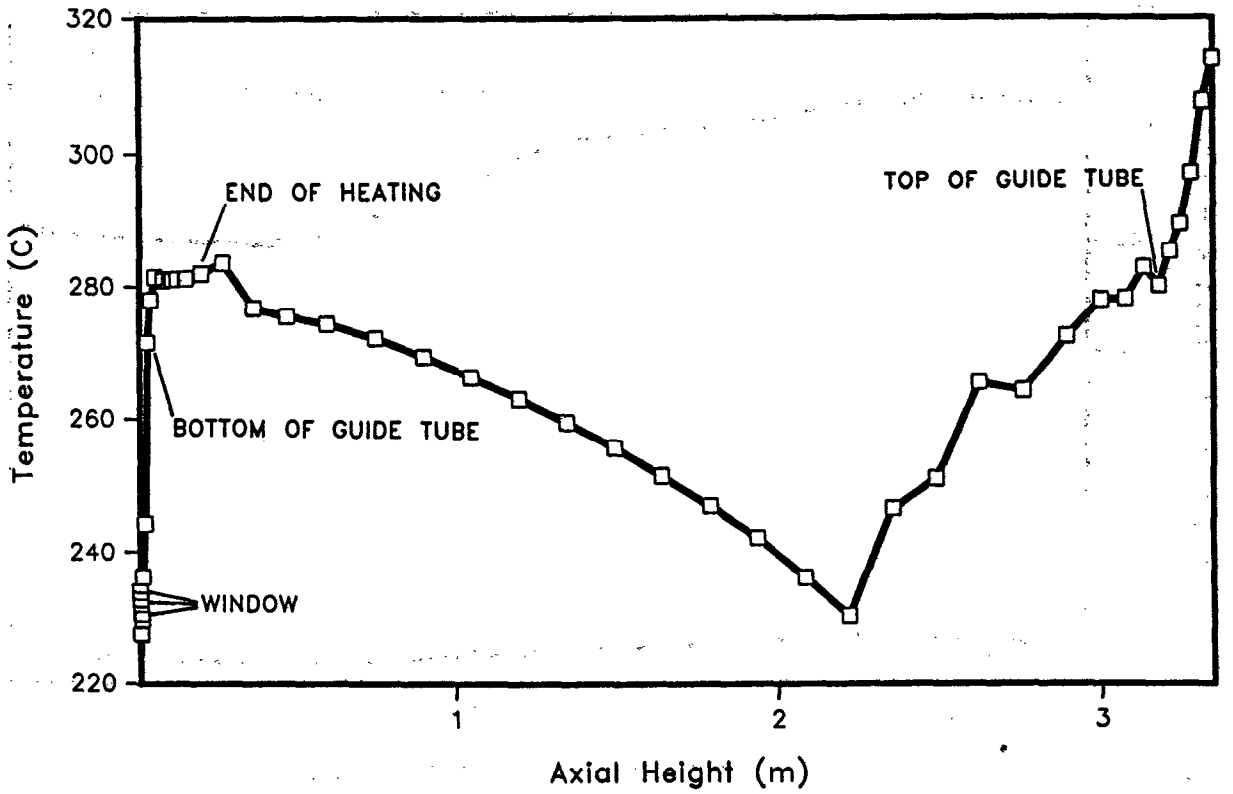

Fig.12 Axial temperature distribution on outer surface of thermally-conducting guide tube

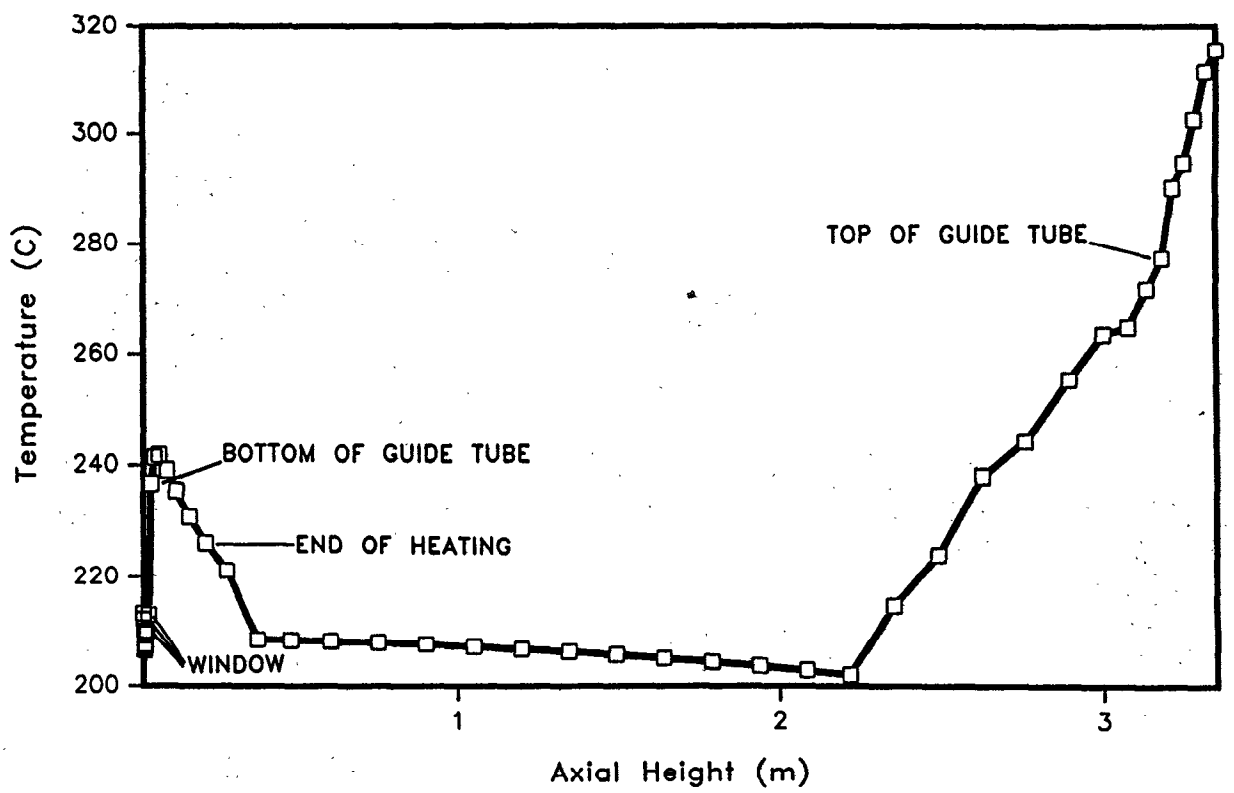

Fig.13 Axial temperature distribution on outer surface of insulated guide tube

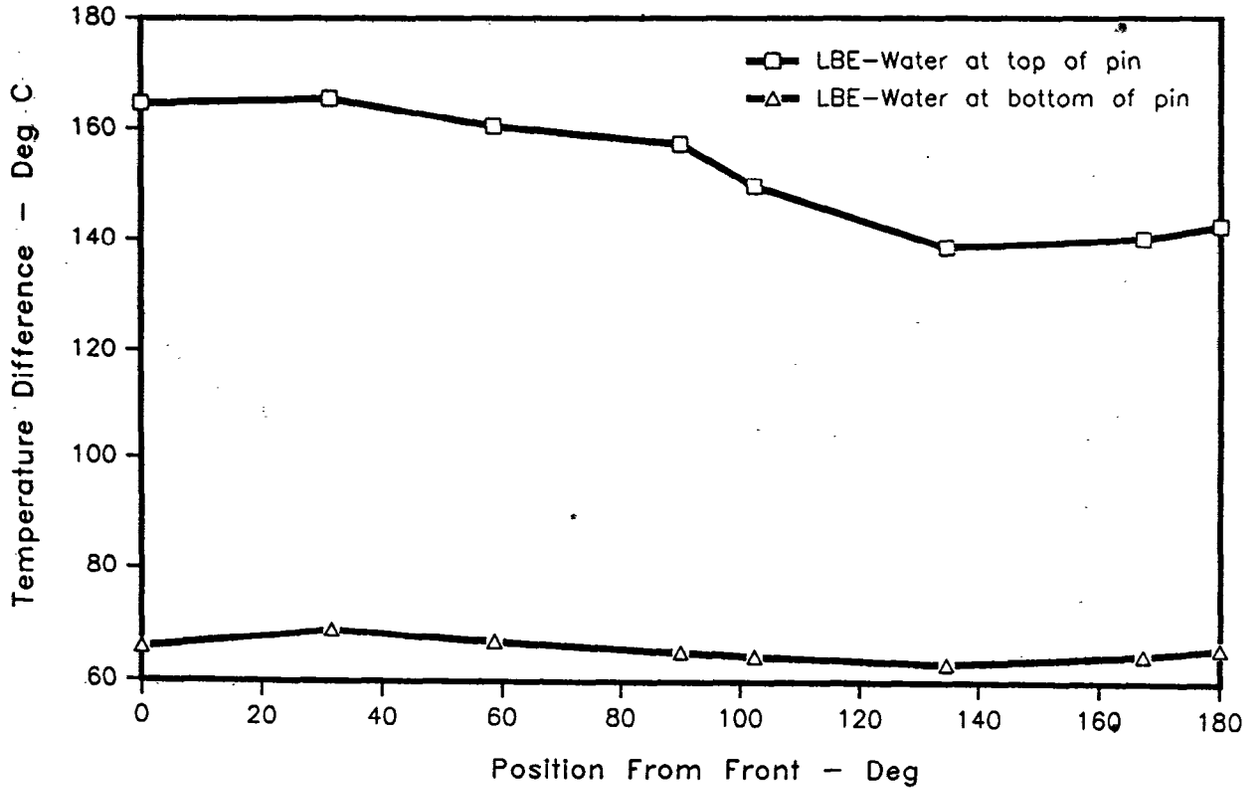

Fig.14 Temperature differences between LBE and Cooling water around circumference of Pin 1 in Fig.15

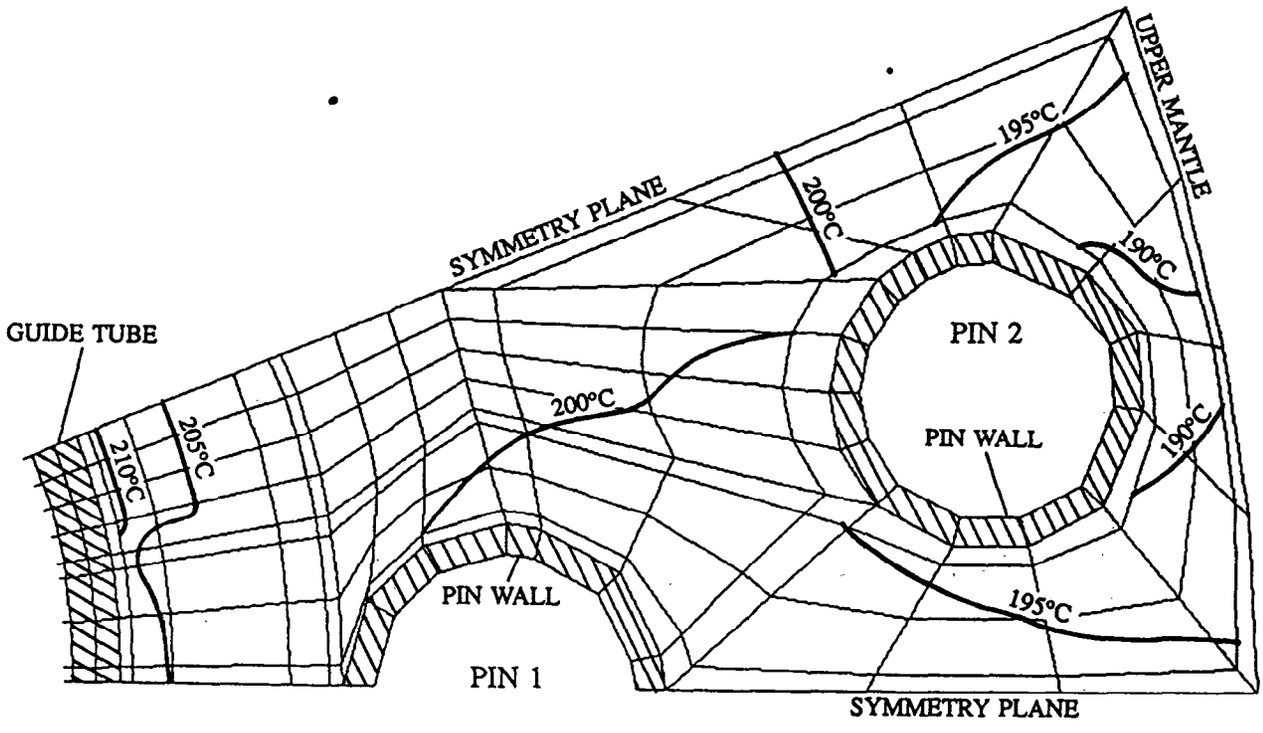

Fig.15 LBE isotherms in target annulus near bottom of cooling pins

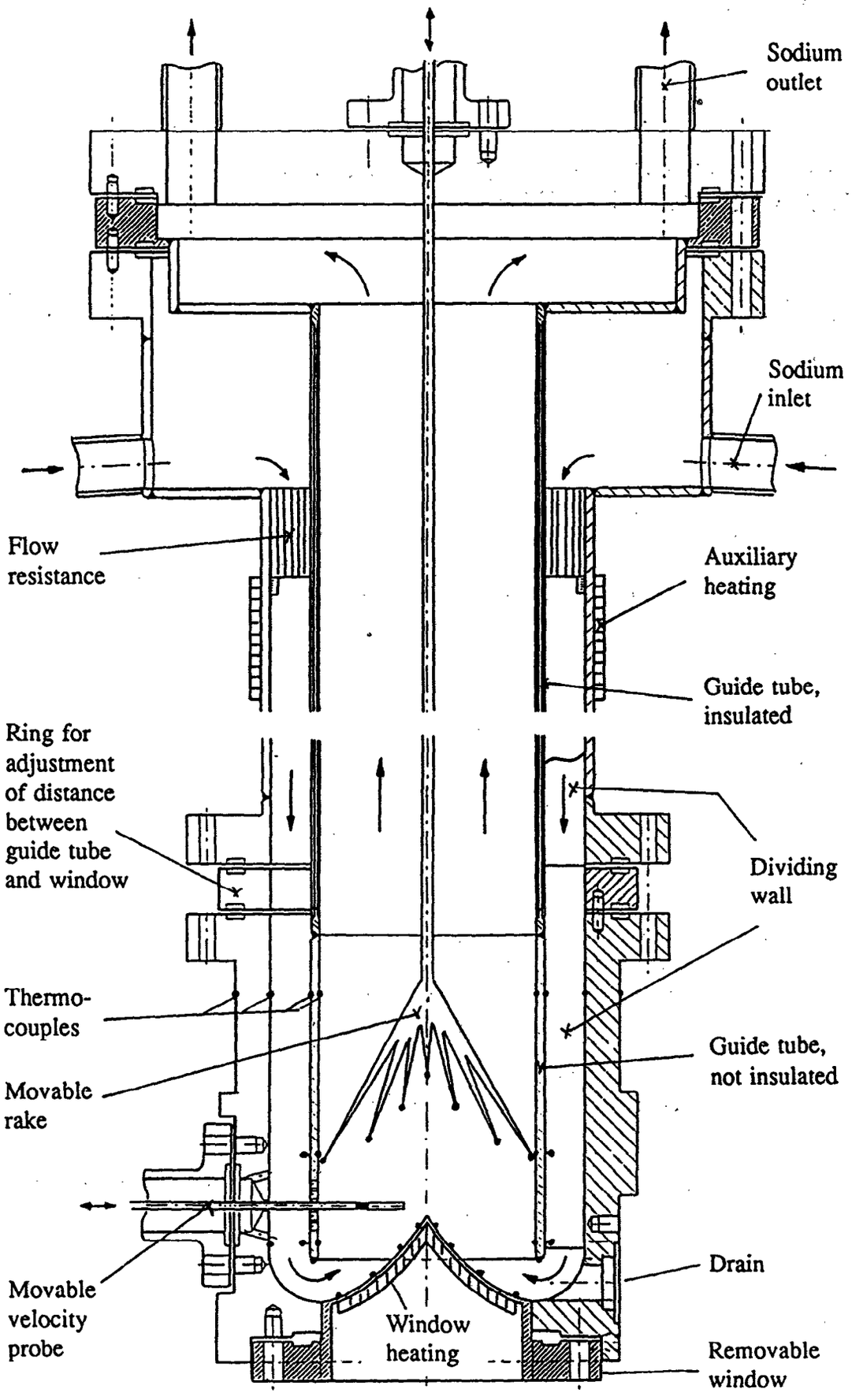

Fig.16 Sketch of TACOS test-section